

## NONLINEAR DYNAMIC ANALYSIS OF VISCOELASTIC MEMBRANES DESCRIBED WITH FRACTIONAL DIFFERENTIAL MODELS

JOHN T. KATSIKADELIS

*School of Civil Engineering, National Technical University of Athens, Athens, Greece*  
*e-mail: jkats@central.ntua.gr*

The dynamic response of an initially flat viscoelastic membrane is investigated. The viscoelastic model is described with fractional order derivatives. The membrane is subjected to surface transverse and inplane dynamic loads. The governing equations are three coupled second order nonlinear partial FDEs (fractional differential equations) of hyperbolic type in terms of the displacement components. These equations are solved using the BEM for fractional partial differential equations developed recently by Katsikadelis. Without excluding other viscoelastic models, the herein employed material is the Kelvin-Voigt model with a fractional order derivative. Numerical examples are presented which not only demonstrate the efficiency of the solution procedure, but also give a better insight into this complicated but very interesting response of structural viscoelastic membranes. It is worth noting that in case of resonance, phenomena similar to those of the Duffing equation are observed.

*Key words:* viscoelastic membranes, nonlinear vibrations, nonlinear fractional differential equations, analog equation method, boundary elements

### 1. Introduction

Membranes made of linear viscoelastic materials are extensively used in modern engineering applications. Various models of the integer differential form have been proposed in order to describe the mechanical behavior of such materials (e.g. Maxwell, Voigt, Kelvin, Zener). Recently, many researchers have shown that viscoelastic models of the differential form with fractional derivatives are in better agreement with the experimental results than the integer derivative models (Stiassnie, 1979; Adolfsson *et al.*, 2005; Meral *et al.*, 2010).

The dynamic response of pure elastic and viscoelastic membranes, using differential constitutive equations of an integer order derivative or hereditary integral type models, have been examined by many investigators (Plaut, 1990; Koivurova and Pramila, 1997; Jevine and MacKintosh, 2002; Wineman, 2007; Goncales *et al.*, 2009). The use of fractional differential models is very limited and is restricted to viscoelastic beams (Galucio *et al.*, 2004) and three dimensional viscoelastic bodies (Schmidt and Gaul, 2002). However, viscoelastic membranes of the fractional type derivative have not been analyzed to date. The reason is plausible as the response of such membranes is described by a system of nonlinear partial FDEs for which an analytical solution is out of question, while numerical methods were not available until lately. Recently, Katsikadelis developed the AEM, which in conjunction with an integral equation approach provides an efficient computational tool for solving linear and nonlinear FDEs, ordinary (Katsikadelis, 2009) and partial (Katsikadelis, 2011). This method is general and paves the way to analyze complicated systems whose response is described by such equations. It has been already employed to solve several problems. Among them, the linear fractional diffusion wave equation in bounded inhomogeneous anisotropic bodies (Katsikadelis, 2008), the response of the inhomogeneous anisotropic viscoelastic bodies (Nerantzaki and Babouskos, 2011) and the nonlinear dynamic

response of viscoelastic plates (Babouskos and Katsikadelis, 2009; Katsikadelis and Babouskos, 2010).

Without excluding other fractional differential models (Nerantzaki and Babouskos, 2011), the employed herein viscoelastic material is described by the Kelvin-Voigt type model with a fractional order derivative

$$\begin{Bmatrix} \sigma_x \\ \sigma_y \\ \tau_{xy} \end{Bmatrix} = \frac{E}{1-\nu^2} \begin{bmatrix} 1 & \nu & 0 \\ \nu & 1 & 0 \\ 0 & 0 & \frac{1-\nu}{2} \end{bmatrix} \begin{Bmatrix} \varepsilon_x + \eta D_c^\alpha \varepsilon_x \\ \varepsilon_y + \eta D_c^\alpha \varepsilon_y \\ \gamma_{xy} + \eta D_c^\alpha \gamma_{xy} \end{Bmatrix} \quad (1.1)$$

where  $E$ ,  $\nu$  are the elastic material constants,  $\eta$  the viscoelastic parameter and  $D_c^\alpha$  the Caputo fractional derivative of the order  $\alpha$  defined as

$$D_c^\alpha u(t) = \begin{cases} \frac{1}{\Gamma(m-\alpha)} \int_0^t \frac{u^{(m)}(\tau)}{(t-\tau)^{\alpha+1-m}} d\tau & \text{for } m-1 < \alpha < m \\ \frac{d^m}{dt^m} u(t) & \text{for } m = \alpha \end{cases} \quad (1.2)$$

where  $m$  is a positive integer. The advantage of this definition is that it permits the assignment of initial conditions which have direct physical significance (Podlubny, 1999). Apparently, the classical derivatives result from Eq. (1.2) for integer values of  $\alpha$ . Thus, Eq. (1.1) for  $\alpha = 1$  gives the constitutive equation for the conventional Kelvin-Voigt model, while for  $\alpha = 0$  the pure elastic model with the elastic modulus  $E^* = E(1 + \eta)$ . The use of fractional differential models, besides their simplicity to formulate the equations of structural viscoelastic systems, exhibit a major advantage, namely they can describe more complicated integer order differential models with few parameters. Nevertheless, due to lack of efficient numerical methods to solve the FDEs, the use of such models, despite their advantages, was very limited to date. The development of efficient numerical methods brings the fractional derivative models in the center of the arena.

The spatial discretization leads to a system of fractional Duffing type equations, which include quadratic terms, beside the cubic ones. Therefore, similar resonance phenomena due to a time harmonic excitation are observed. The nonlinear resonance of the membrane under a harmonic force is studied by integrating the equations of motion over a long time, until a steady-state solution is obtained. The stable solutions (attractors) can be obtained by an appropriate selection of the initial conditions. However, this method may need a very long time to reach a stable solution, while it is impossible to obtain the unstable ones. More efficient methods, such as the harmonic balance method, the Poincare map and arc-length methods for periodic solutions (Amabili, 2008) have been employed to obtain numerical results. The dominant resonance appears when the excitation frequency is close to the lower natural frequency of the membrane structure. Secondary resonances occur for specific values of the excitation frequency, which may be lower (superharmonic resonance) or greater (subharmonic resonance) than the first natural frequency. In all cases, the amplitude of vibration increases, while jump and hysteretic phenomena appear due to the nonlinear character of the problem. Such behavior has been reported previously in many single and multi-degree of freedom nonlinear systems using analytical and approximate techniques (Nayfeh and Mook, 1979). A membrane of an arbitrary shape is analyzed. Free vibrations as well as forced vibrations under step and harmonic loads are studied. The obtained numerical results validate the efficiency of the solution method and allow one to draw useful conclusions for the dynamic response of viscoelastic membranes.

## 2. Problem statement and governing equations

We consider a thin flexible initially flat elastic membrane of thickness  $h$  and mass density  $\rho$  consisting of a homogeneous linearly viscoelastic material occupying the two-dimensional, in general multiply connected, domain  $\Omega$  in the  $x, y$  plane. The membrane is prestressed either by the imposed displacement  $u_n^*, v_t^*$  or by external forces  $N_n^*, N_t^*$  acting along the boundary  $\Gamma$ . Moderate large deflections result from nonlinear kinematic relations, which retain the square of the slopes of the deflection surface, while the strain components remain still small compared with the unity. This theory is good for considerably large deflections with the exception in the vicinity of the boundary where the stress resultants of the finite deformation of the membrane should be considered to satisfy the equilibrium and explain the folding near the edge. Thus, the strain components are given as

$$\varepsilon_x = u_{,x} + \frac{1}{2}w_{,x}^2 \quad \varepsilon_y = v_{,y} + \frac{1}{2}w_{,y}^2 \quad \gamma_{xy} = u_{,y} + v_{,x} + w_{,x}w_{,y} \quad (2.1)$$

where  $u = u(x, y, t)$ ,  $v = v(x, y, t)$  are the inplane (membrane) displacement components and  $w = w(x, y, t)$  the transverse one. The membrane is subjected to the transverse load  $p_z = p_z(x, y, t)$  and the inplane loads  $p_x = p_x(x, y, t)$  and  $p_y = p_y(x, y, t)$ .

On the basis of Eqs. (1.1) and (2.1) the stress resultants are written as

$$\bar{N}_x = N_x + D_c^\alpha N_x \quad \bar{N}_y = N_y + D_c^\alpha N_y \quad \bar{N}_{xy} = N_{xy} + D_c^\alpha N_{xy} \quad (2.2)$$

where

$$\begin{aligned} N_x &= C \left[ u_{,x} + \nu v_{,y} + \frac{1}{2}(w_{,x}^2 + \nu w_{,y}^2) \right] & N_y &= C \left[ \nu u_{,x} + v_{,y} + \frac{1}{2}(\nu w_{,x}^2 + w_{,y}^2) \right] \\ N_{xy} &= C \frac{1-\nu}{2} (u_{,y} + v_{,x} + w_{,x}w_{,y}) \end{aligned} \quad (2.3)$$

$C = Eh/(1 - \nu^2)$  is the membrane stiffness.

The governing equations result by taking the equilibrium of the membrane element in a slightly deformed configuration. This yields

$$\begin{aligned} \bar{N}_{x,x} + \bar{N}_{xy,y} - \rho h \ddot{u} &= -p_x & \bar{N}_{y,y} + \bar{N}_{xy,x} - \rho h \ddot{v} &= -p_y \\ \bar{N}_x w_{,xx} + 2\bar{N}_{xy} w_{,xy} + \bar{N}_y w_{,yy} - p_x w_{,x} - p_y w_{,y} - \rho h \ddot{w} + \rho h \ddot{u} w_{,x} + \rho h \ddot{v} w_{,y} &= -p_z \end{aligned} \quad (2.4)$$

Without restricting the generality, we consider displacement boundary conditions on  $\Gamma$

$$u_n = u_n^* \quad u_t = v_t^* \quad w = w^* \quad (2.5)$$

Inserting Eqs. (2.2) combined with Eqs. (2.3) in Eqs. (2.4), we obtain equations governing the response of the membrane in terms of the displacements in  $\Omega$

$$\begin{aligned} &C \left\{ \left[ u_{,x} + \nu v_{,y} + \frac{1}{2}(w_{,x}^2 + \nu w_{,y}^2) \right] + \eta D_c^\alpha \left[ u_{,x} + \nu v_{,y} + \frac{1}{2}(w_{,x}^2 + \nu w_{,y}^2) \right] \right\}_{,x} \\ &+ C \frac{1-\nu}{2} \{ (u_{,y} + v_{,x} + w_{,x}w_{,y}) + \eta D_c^\alpha (u_{,y} + v_{,x} + w_{,x}w_{,y}) \}_{,y} - \rho h \ddot{u} = -p_x \\ &C \frac{1-\nu}{2} \{ (u_{,y} + v_{,x} + w_{,x}w_{,y}) + \eta D_c^\alpha (u_{,y} + v_{,x} + w_{,x}w_{,y}) \}_{,x} \\ &+ C \left\{ \left[ \nu u_{,x} + v_{,y} + \frac{1}{2}(\nu w_{,x}^2 + w_{,y}^2) \right] + \eta D_c^\alpha \left[ \nu u_{,x} + v_{,y} + \frac{1}{2}(\nu w_{,x}^2 + w_{,y}^2) \right] \right\}_{,y} - \rho h \ddot{v} = -p_y \\ &C \left\{ \left[ u_{,x} + \nu v_{,y} + \frac{1}{2}(w_{,x}^2 + \nu w_{,y}^2) \right] + \eta D_c^\alpha \left[ u_{,x} + \nu v_{,y} + \frac{1}{2}(w_{,x}^2 + \nu w_{,y}^2) \right] \right\} w_{,xx} \\ &+ C(1-\nu) \{ (u_{,y} + v_{,x} + w_{,x}w_{,y}) + \eta D_c^\alpha (u_{,y} + v_{,x} + w_{,x}w_{,y}) \} w_{,xy} \\ &+ C \left\{ \left[ \nu u_{,x} + v_{,y} + \frac{1}{2}(\nu w_{,x}^2 + w_{,y}^2) \right] + \eta D_c^\alpha \left[ \nu u_{,x} + v_{,y} + \frac{1}{2}(\nu w_{,x}^2 + w_{,y}^2) \right] \right\} w_{,yy} \\ &- p_x w_{,x} - p_y w_{,y} - \rho h \ddot{w} + \rho h \ddot{u} w_{,x} + \rho h \ddot{v} w_{,y} = -p_z \end{aligned} \quad (2.6)$$

Equations (2.6) are subjected besides boundary conditions (2.5) also to the initial conditions

$$\begin{aligned} u(x, y, 0) &= f_1(x, y) & \dot{u}(x, y, 0) &= g_1(x, y) \\ v(x, y, 0) &= f_2(x, y) & \dot{v}(x, y, 0) &= g_2(x, y) \\ w(x, y, 0) &= f_3(x, y) & \dot{w}(x, y, 0) &= g_3(x, y) \end{aligned} \quad (2.7)$$

Equations (2.6) constitute a system of three coupled nonlinear partial FDEs of hyperbolic type that are solved using the BEM presented in Katsikadelis (2011), which for the problem at hand is adjusted as in the following.

### 3. The BEM solution

Equations (2.6) are of the second order with regard to the spatial derivatives, thus according to the *principle of the analog equation* they can be replaced by the equations

$$\nabla^2 u = b^{(1)}(\mathbf{x}, t) \quad \nabla^2 v = b^{(2)}(\mathbf{x}, t) \quad \nabla^2 w = b^{(3)}(\mathbf{x}, t) \quad (3.1)$$

where  $\mathbf{x} = \{x, y\} \in \Omega$ ,  $t > 0$  and  $b^{(i)}(\mathbf{x}, t)$ ,  $i = 1, 2, 3$  represent time dependent fictitious sources, unknown in the first instance. The solution to Eq. (3.1)<sub>1</sub> is given in integral form (Katsikadelis, 2002)

$$\varepsilon u(\mathbf{x}, t) = \int_{\Omega} u^* b \, d\Omega - \int_{\Gamma} (u^* q - q^* u) \, ds \quad \mathbf{x} \in \Omega \cup \Gamma \quad (3.2)$$

in which  $q = u_{,n}$ ;  $u^* = \ell nr/2\pi$  is the fundamental solution to Eq. (3.1) and  $q^* = u_{,n}^*$  its derivative normal to the boundary with  $r = \|\xi - \mathbf{x}\|$ ,  $\mathbf{x} \in \Omega \cup \Gamma$  and  $\xi \in \Gamma$ ;  $\varepsilon$  is the free term coefficient ( $\varepsilon = 1$  if  $\mathbf{x} \in \Omega$ ,  $\varepsilon = \omega/2\pi$  if  $\mathbf{x} \in \Gamma$  and  $\varepsilon = 0$  if  $\mathbf{x} \notin \Omega \cup \Gamma$ ) and  $\omega$  is the interior angle between the tangents of the boundary at the point  $\mathbf{x}$ ;  $\varepsilon = 1/2$  for points where the boundary is smooth. Eq. (3.2) is solved numerically using the BEM. The boundary integrals are approximated using  $N$  constant boundary elements, whereas the domain integrals are approximated using  $M$  linear triangular cells. The domain discretization is performed automatically using the Delaunay triangulation. Since the fictitious source is not defined on the boundary, the nodal points of the triangles adjacent to the boundary are placed on their sides (Fig. 1). Thus, after discretization

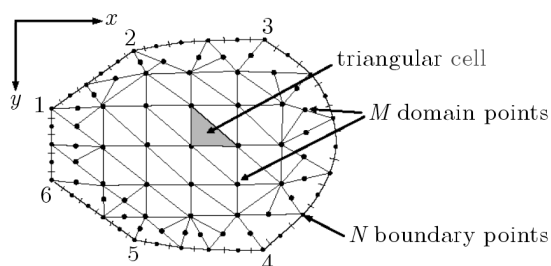


Fig. 1. Boundary and domain discretization

and application Eq. (3.2) at the  $N$  boundary nodal points, we obtain

$$\mathbf{H}\mathbf{u} = \mathbf{G}\mathbf{q} + \mathbf{A}\mathbf{b}^{(1)} \quad (3.3)$$

where  $\mathbf{H}$ ,  $\mathbf{G}$  are  $N \times N$  known coefficient matrices originating from the integration of the kernel functions on the boundary and  $\mathbf{A}$  is an  $N \times M$  coefficient matrix originating from the integration of the kernel function on the domain cells;  $\mathbf{u}$ ,  $\mathbf{q}$  are the vectors of the  $N$  nodal displacements

and slopes and  $\mathbf{b}^{(1)}$  the nodal values of the fictitious source at the  $M$  domain nodal points, all at time  $t$ . The derivatives of  $u(\mathbf{x}, t)$  inside  $\Omega$  are obtained by direct differentiation of Eq. (3.2) with  $\varepsilon = 1$ . Further, by applying Eq. (3.2) and its derivatives at the domain nodal points and making use of Eq. (3.3) combined with the boundary conditions to eliminate the boundary quantities, we can express  $\mathbf{u}(t)$  and its derivatives at the domain nodal points in terms of the fictitious source

$$\mathbf{u}_{,pq}(t) = \mathbf{S}_{,pq} \mathbf{b}^{(1)}(t) + \mathbf{s}^{(1)}_{,pq} \quad p, q = 0, x, y \tag{3.4}$$

Similarly, we obtain

$$\mathbf{v}_{,pq}(t) = \mathbf{S}_{,pq} \mathbf{b}^{(2)}(t) + \mathbf{s}^{(2)}_{,pq} \quad p, q = 0, x, y \tag{3.5}$$

and

$$\mathbf{w}_{,pq}(t) = \mathbf{S}_{,pq} \mathbf{b}^{(3)}(t) + \mathbf{s}^{(3)}_{,pq} \quad p, q = 0, x, y \tag{3.6}$$

where  $\mathbf{S}_{,pq}$  are known  $M \times M$  matrices and  $\mathbf{s}^{(i)}_{,pq}$  known vectors. For homogeneous boundary conditions, we have  $\mathbf{s}^{(i)}_{,pq} = 0$ . The notation  $\mathbf{u}_{,pq}$  designates  $\mathbf{u}_{,00} = \mathbf{u}$ ,  $\mathbf{u}_{,x0} = \mathbf{u}_{,x}$  etc. Applying now Eqs. (2.6) at the  $M$  domain nodal points and substituting the involved derivatives from Eqs. (3.4)-(3.6), we obtain

$$\mathbf{M}^{(i)} \ddot{\mathbf{b}}^{(i)} + \mathbf{F}^{(i)}(\mathbf{b}^{(i)}, D_c^\alpha \mathbf{b}^{(i)}) = \mathbf{f}^{(i)} \quad i = 1, 2, 3 \tag{3.7}$$

where  $\mathbf{M}^{(i)}$  are  $M \times M$  consistent mass matrices,  $\mathbf{F}^{(i)}$  are  $M \times 1$  vectors whose elements depend nonlinearly on the arguments and  $\mathbf{f}^{(i)}$  are known load vectors. Using Eqs. (3.4)-(3.6), initial conditions (2.7) for  $\mathbf{b}^{(i)}$  become

$$\mathbf{b}^{(i)}(0) = \mathbf{S}^{-1}(\mathbf{f}_i - \mathbf{s}^{(i)}) \quad \dot{\mathbf{b}}^{(i)}(0) = \mathbf{S}^{-1} \mathbf{g}_i \tag{3.8}$$

Equations (3.7) constitute a system of  $3M$  three-term nonlinear FDEs, which are solved using the time step numerical procedure developed by Katsikadelis (2009). The use, however, of all degrees of freedom, i.e.  $3M$ , may be computationally costly and in some cases inefficient due to the large number of the time dependent variables  $b_k^{(i)}(t)$ . To overcome this difficulty in this investigation, the number of degrees of freedom is reduced using the Ritz transformation, namely

$$\mathbf{b}^{(i)} = \mathbf{\Psi}^{(i)} \mathbf{z}^{(i)} \tag{3.9}$$

where  $z_k^{(i)}(t)$ , ( $k = 1, \dots, L < M$ ) are new time dependent parameters and  $\mathbf{\Psi}^{(i)}$  is the  $M \times L$  transformation matrix. In this investigation the eigenmodes of the linear problem are employed as Ritz vectors.

## 4. Numerical examples

### 4.1. Free and forced vibrations under suddenly applied uniform load

The dynamic response of the viscoelastic membrane shown in Fig. 2 has been studied. The boundary of the domain is defined by the curve

$$r = \sqrt{ab} \sqrt[4]{\frac{\left(\frac{\cos \theta}{b}\right)^2 + \left(\frac{\sin \theta}{a}\right)^2}{\left(\frac{\cos \theta}{a}\right)^2 + \left(\frac{\sin \theta}{b}\right)^2}} \quad 0 \leq \theta \leq 2\pi$$

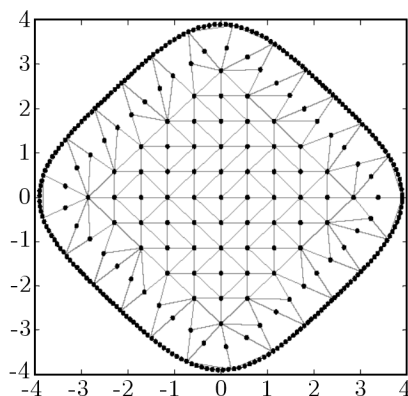


Fig. 2. Boundary and domain nodal points of the membrane

The membrane is prestressed by  $u_n = 0.2$  m in the direction normal to the boundary and  $u_t = 0$  m in the tangential direction. The employed data are:  $a = 3$ ,  $b = 1.3$ ;  $h = 0.002$  m,  $\rho/h = 5000$  kg/m<sup>3</sup>,  $E = 1.1 \cdot 10^5$  kN/m<sup>2</sup>,  $\nu = 0.3$ . The results were obtained using  $N = 210$  boundary elements and  $M = 106$  internal collocation points resulting from 164 linear triangular domain cells.

Firstly, the influence of the inplane inertia forces is investigated. The membrane is assumed purely elastic and is subjected to a transverse load  $p_z = 2H(t)$  kN/m<sup>2</sup>. Figures 3a,b,c present the time history of the transverse displacement  $w(0,0,t)$  at the center of the membrane, the inplane displacement  $u(-1.741,0,t)$  and the membrane force  $N_x(-1.741,0,t)$ , respectively, for the cases where the membrane inertia forces are taken into account and neglected. Apparently, the influence of the membrane inertia forces is negligible. Moreover, Figs. 4a,b show the deflection  $w(0,0,t)$  and the inplane displacement  $u(-1.741,0,t)$  for various numbers of linear modes employed in the Ritz method for reduction of the degrees of freedom as compared with the results of the unreduced system. It is noteworthy that the use of more than 20 modes changes the results negligibly. This reduction is significant because it allows us to obtain accurate results using a small number of degrees of freedom.

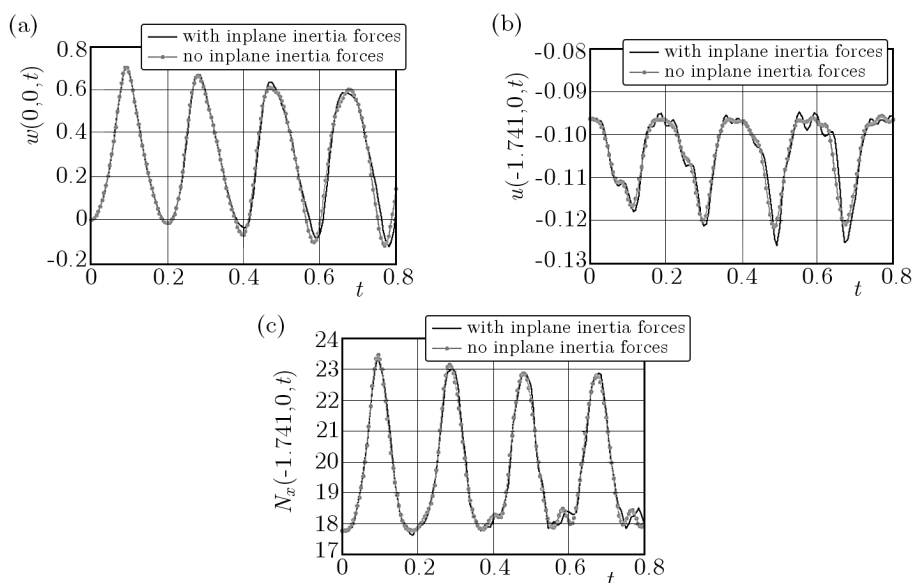


Fig. 3. Time history of (a) transverse displacements  $w(0,0,t)$ , (b) inplane displacement  $u(-1.741,0,t)$  and (c) membrane force  $N_x(-1.741,0,t)$

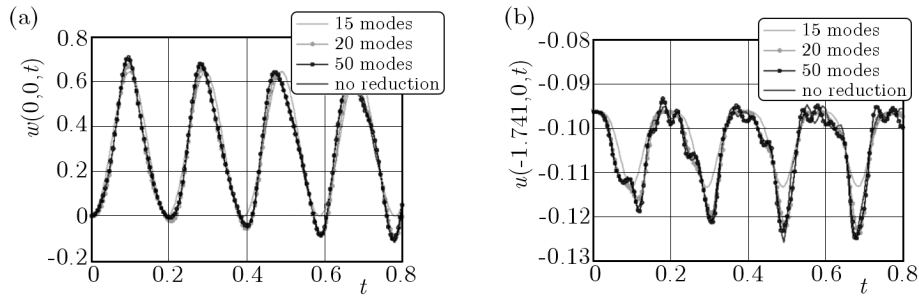


Fig. 4. (a) Transverse displacement  $w(0,0,t)$  and (b) inplane displacement  $u(-1.741,0,t)$  for different numbers of the linear modes for reduction of degrees of freedom

Next, the free vibrations of the elastic ( $\eta = 0$ ) and the viscoelastic membrane ( $\eta = 0.2$ ) are studied. The initial conditions are  $w(x,y,0)$  the deflection of the membrane due to a uniform static load  $p_z = 1.0 \text{ kN/m}^2$  and  $\dot{w}(x,y,0) = 0$ . The results were obtained using 20 linear modes for the Ritz reduction. Figure 5 shows the response of the membrane for the elastic ( $\eta = 0$ ) and viscoelastic ( $\alpha = 1, \eta = 0.2$ ) material.

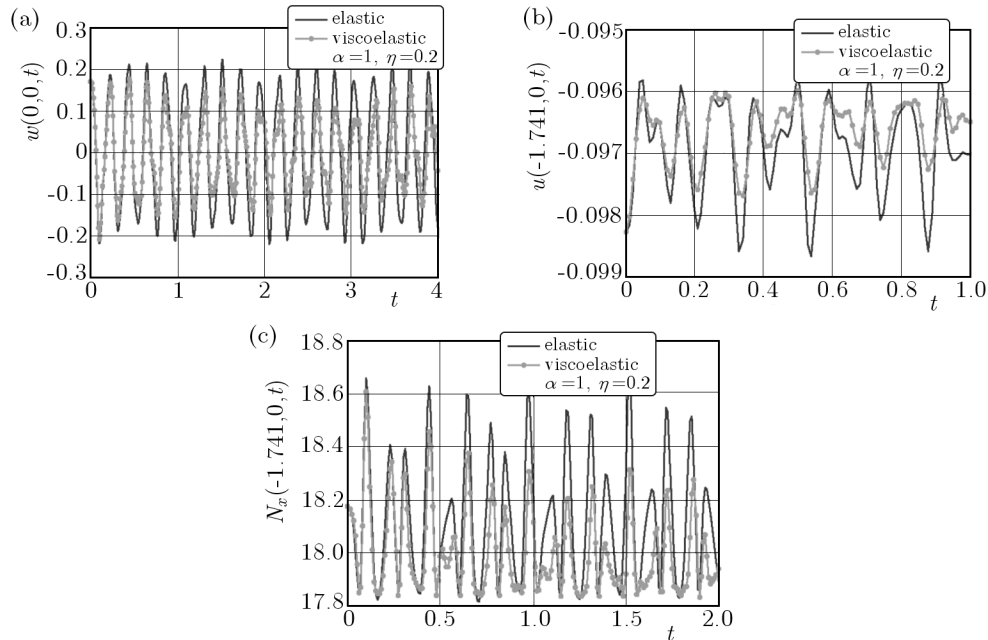


Fig. 5. Time history of (a)  $w(0,0,t)$ , (b)  $u(-1.741,0,t)$ , (c)  $N_x(-1.741,0,t)$  for elastic ( $\eta = 0$ ) and viscoelastic ( $\alpha = 1, \eta = 0.2$ ) material

Finally, the forced vibrations of the viscoelastic membrane are studied. The membrane is subjected to a transverse load  $p_z = 1.0H(t) \text{ kN/m}^2$ . The results were obtained using 20 linear modes for reduction. Figure 6 presents the time history of the membrane for various values of the order of the fractional derivative of the fractional Kelvin-Voigt type model. This figure shows how the fractional order influences the viscoelastic response. Figure 7a shows the deflection  $w(0,0,t)$  for the elastic and viscoelastic material as compared with the static deflection, while Fig. 7b depicts the phase plane of the deflection at the center for  $\alpha = 0.5, \eta = 0.5$ .

#### 4.2. Forced vibrations under harmonic load. Resonance

The dynamic response of the viscoelastic membrane of example 4.1 under the transverse harmonic excitation  $p_z = p_0 \sin(\Omega t)$  has been studied. The results were obtained using  $N = 210$

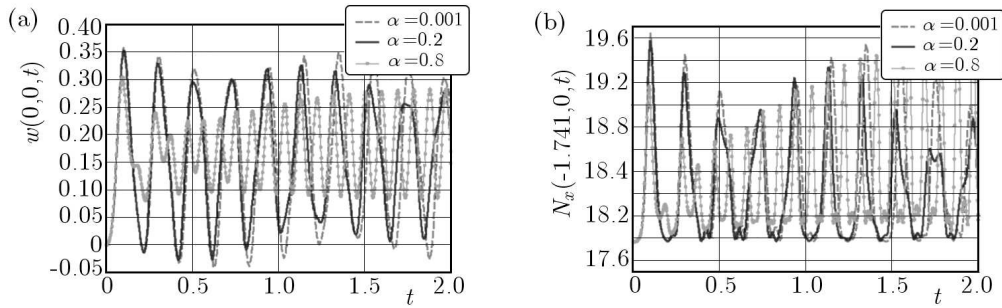


Fig. 6. Time history of (a)  $w(0,0,t)$  and (b)  $N_x(-1.741,0,t)$  for various values of the order  $\alpha$  ( $\eta = 0.5$ )

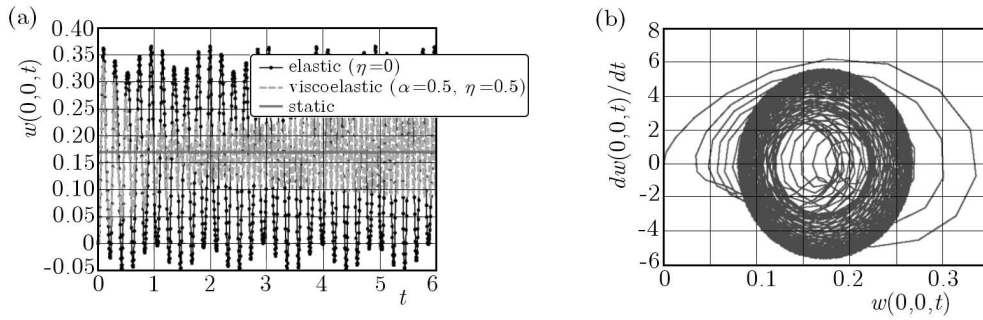


Fig. 7. (a) Time history of deflection at the center of a viscoelastic membrane ( $\alpha = 0.5, \eta = 0.5$ ) and (b) phase

boundary elements and  $M = 122$  internal collocation points resulting from 193 linear triangular cells and 10 linear mode shapes for the reduction of the degrees of freedom.

First, we study the response of the conventional Kelvin-Voigt viscoelastic model ( $\alpha = 1$ ) when the external frequency  $\Omega$  is close to the lower natural frequency of the linear membrane, which was found  $\omega = 0.916$ . Figure 8a presents the amplitude of vibration (steady state response) at the center of the membrane for the nonlinear problem together with that of the

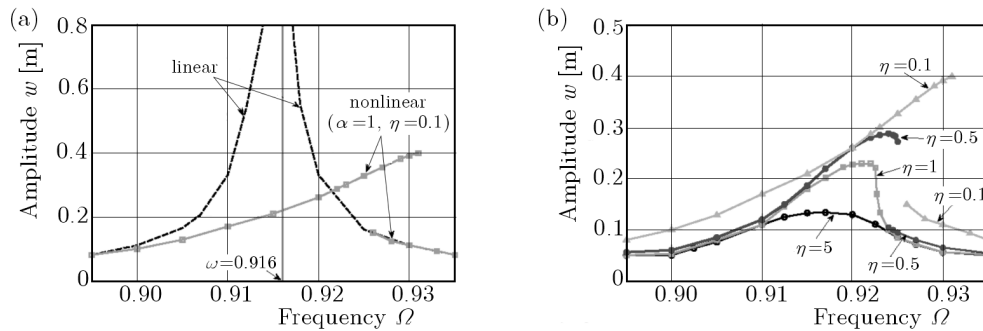


Fig. 8. Amplitude-frequency curves at the center of the membrane for the linear and nonlinear problem (a) and for various values of the viscous parameter for the classical Kelvi-Voigt model ( $\alpha = 1$ )

linear undamped membrane (the nonlinear terms have been neglected). It is observed that the amplitude of vibrations increase as the external frequency  $\Omega$  approaches the natural frequency. However, the amplitude curves of the nonlinear problem move to right, indicating hardening nonlinear behavior, while two stable solutions are observed for some values of the excitation frequency. Moreover, due to the viscoelastic material, the vibrations are bounded contrary to the linear membrane problem. Figure 8b presents the amplitude-frequency curves for various values of the viscous parameter  $\eta$ . The amplitude of vibrations increases as the viscous parameter decreases. For  $\eta < 1$  a jump phenomenon appears and two stable solutions are observed.

Figure 9a presents the time history of the deflection at the center of the membrane for two values of the external frequency, a little before and after the jump. The frequency is changed at  $t = 2400$  s. Figure 9b presents the influence of the initial conditions on the steady state response of the membrane.

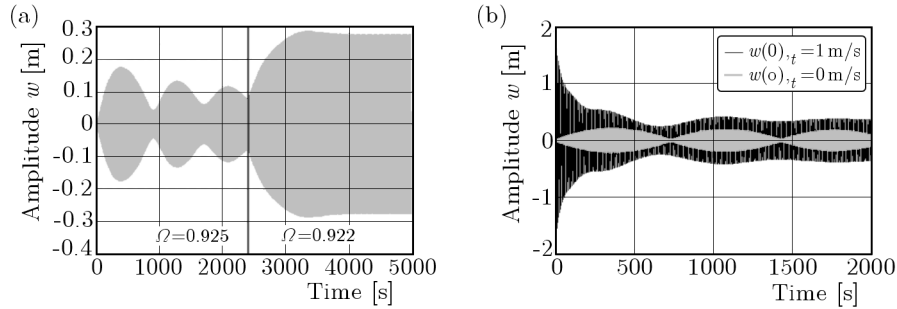


Fig. 9. Time history of the central deflection for (a) two values of the external frequency ( $\alpha = 1$ ,  $\eta = 0.5$ ,  $p_0 = 0.01$ ) and (b) two values of the initial velocity ( $\alpha = 1$ ,  $\eta = 0.1$ ,  $\Omega = 0.927$ ,  $p_0 = 0.12$ )

Similar jump phenomena appear for certain values of the excitation frequency when the amplitude  $p_0$  of the external harmonic load varies within a certain interval. This is shown in Fig. 10, where two stable solutions appear for two values of the external frequency ( $\Omega_1 = 0.922$ ,  $\Omega_2 = 0.927$ ) with varying the amplitude  $p_0$ .

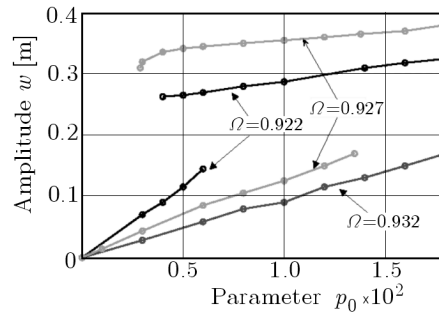


Fig. 10. Amplitude of the response of the membrane as a function of the external amplitude  $p_0$

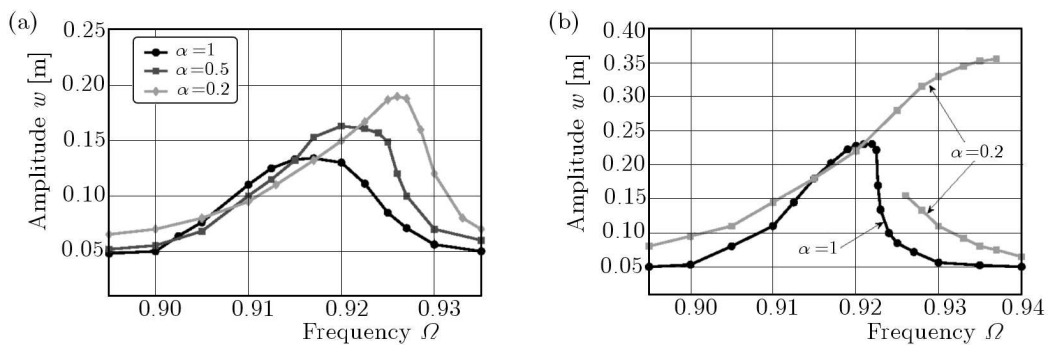


Fig. 11. Amplitude-frequency curves for: (a) various values of the fractional derivative  $\alpha$  ( $\eta = 5$ ), (b) two values of the fractional derivative  $\alpha$  ( $\eta = 1$ )

Next, we study the response of the fractional Kelvin-Voigt model. Figures 11a and 11b present the amplitude of the steady state response at the center of the membrane for various values of the order of the fractional derivative  $\alpha$  and for two values of the viscous parameter ( $\eta = 5$  and  $\eta = 1$ ). It is observed that the amplitude of the steady state response increases as

the fractional derivative decreases. For  $\alpha = 0.2$ ,  $\eta = 1$  and for appropriate initial conditions, two stable solutions appear.

## 5. Conclusions

The governing equations describing the nonlinear dynamic response of viscoelastic membranes made of fractional type derivative viscoelastic materials are derived. The resulting nonlinear partial fractional differential equations are solved using the BEM developed recently by Katsikadelis. The membrane may have an arbitrary shape. Free and forced vibrations are studied. The response under a harmonic excitation is also highlighted. Various important conclusions are drawn pertaining to the nonlinear dynamic response of viscoelastic membranes. Among them:

- The membrane inertia forces have a negligible effect.
- The semidiscretized equations of motion constitute a system of coupled Duffing type ordinary FDEs. Therefore, similar resonance phenomena due to the time harmonic excitation are observed.
- The jump phenomena are bounded and they are considerably influenced by the order of the fractional derivative in the Kelvin-Voigt. Moreover, a unique stable position can result for an appropriate value of the order of the fractional derivative. Thus, the use of membranes made of viscoelastic materials enables them to avoid disastrous phenomena due to resonance.

In closing, the presented method provides an efficient computational tool to analyze nonlinear viscoelastic membranes described by realistic models and enables the investigator to understand their complicated dynamic response. Moreover, the subject of nonlinear viscoelastic membranes involves interesting and important applications, computational issues and applied mathematics.

## References

1. ADOLFSSON K., ENELUND M., OLSSON P., 2005, On the fractional order model of viscoelasticity, *Mechanics of Time-Dependent Materials*, **9**, 15-34
2. AMABILI M., 2008, *Nonlinear Vibrations and Stability of Shells and Plates*, Cambridge University Press
3. BABOUSKOS N., KATSIKADELIS J.T., 2009, Nonlinear vibrations of viscoelastic plates of fractional derivative type. An AEM solution, *Open Mechanics Journal*, **3**, 25-44
4. GALUCIO A.C., DEU J.F., OHAYON R., 2004, Finite element formulation of viscoelastic sandwich beams using fractional derivative operators, *Computational Mechanics*, **33**, 282-291
5. GONCALES P.B., SOARES R.M., PAMPLONA D., 2009, Nonlinear vibrations of a radially stretched circular hyperelastic membrane, *J. of Sound and vibration*, **327**, 231-248
6. JEVINE A.J., MACKINTOSCH F.C., 2002, Dynamics of viscoelastic membranes, *Physical Review*, **E 66**, 061606
7. KATSIKADELIS J.T., 2002, *Boundary Elements. Theory and Applications*, Elsevier, Oxford, U.K.
8. KATSIKADELIS J.T., 2008, The fractional wave-diffusion equation in bounded inhomogeneous anisotropic media. An AEM solution, [In:] *Advances in Boundary Element Methods*, G.D. Manolis, D. Polyzos (Eds.), 255-276, Springer Science, Dordrecht, Netherlands
9. KATSIKADELIS J.T., 2009, Numerical solution of multi-term fractional differential equations, *ZAMM Zeitschrift für Angewandte Mathematik und Mechanik*, **89**, 7, 593-608
10. KATSIKADELIS J.T., 2011, The BEM for Numerical solution of partial fractional differential equations, *Computers and Mathematics with Applications*, **62**, 891-901

11. KATSIKADELIS J.T., BABOUSKOS N., 2010, Post-buckling analysis of viscoelastic plates with fractional derivative models, *Engineering Analysis with Boundary Elements*, **34**, 1038-1048
12. KOIVUROVA H., PRAMILA A., 1997, Nonlinear vibration of axially moving membrane by finite element method, *Computational Mechanics*, **20**, 573-581
13. MERAL F.C., ROYSTON T.J., MAGIN R., 2010, Fractional calculus in viscoelasticity: An experimental study, *Commun. Nonlinear Sci. Numer. Simulat.*, **15**, 939-945
14. NAYFEH A.H., MOOK D.T., 1979, *Nonlinear Oscillations*, New York, Wiley
15. NERANTZAKI M.S., BABOUSKOS N., 2011, Analysis of inhomogeneous anisotropic viscoelastic bodies described by multi-parameter fractional differential constitutive models, *Computers and Mathematics with Applications*, **62**, 891-901
16. PLAUT R., 1990, Parametric excitation of an inextensible, air-inflated, cylindrical membrane, *Int. J. Non-linear Mechanics*, **25**, 253-262
17. PODLUBNY I., 1999, *Fractional Differential Equations*, Academic Press, New York
18. SCHMIDT A., GAUL L., 2002, Finite element formulation of viscoelastic constitutive equations using fractional time derivatives, *Nonlinear Dynamics*, **29**, 1/4, 37-55
19. STIASSNIE M., 1979, On the application of fractional calculus for the formulation of viscoelastic models, *Applied Mathematical Modeling*, **3**, 300-302
20. WINEMAN A., 2007, Nonlinear viscoelastic membranes, *Computers and Mathematics with Applications*, **53**, 168-181

### **Analiza nieliniowej dynamiki lepko-sprężystych powłok opisanych modelem o pochodnej ułamkowej**

#### Streszczenie

W pracy przedstawiono analizę dynamiki płaskiej powłoki lepko-sprężystej po wstępnym ugięciu. Reologiczny model materiału powłoki opisano równaniem o pochodnych ułamkowych. Powłokę poddano płaskiemu, poprzecznemu obciążeniu zewnętrznemu. Zagadnienie dynamiki ujęto układem trzech sprzężonych nieliniowych równań różniczkowych typu hiperbolicznego o pochodnych ułamkowych. Równania rozwiązano metodą elementów brzegowych (BEM) sformułowaną przez autora właśnie dla układów opisanych pochodnymi ułamkowymi. W prezentowanej pracy założono, że powłoka wykonana jest z lepko-sprężystego materiału Kelvina-Voigta o pochodnej ułamkowej, choć samo sformułowanie BEM nie wyklucza możliwości analizy innych modeli reologicznych. Przedstawiono kilka przykładów symulacji numerycznych pokazujących efektywność zastosowanej metody rozwiązywania oraz dających lepszy obraz interesującej, lecz skomplikowanej dynamiki lepko-sprężystych powłok. Warto również podkreślić, że w warunkach rezonansowych odnotowano zjawiska podobne do obserwowanych w układzie Duffinga.

*Manuscript received November 7, 2011, accepted for print February 6, 2012*